JOURNAL OF ENVIRONMENTAL SCIENCES 104 (2021) 430–443

Available online at www.sciencedirect.com

ScienceDirect

www.elsevier.com/locate/jes

JES JOURNAL OF ENVIRONMENTAL SCIENCES

www.jesc.ac.cn

Optimized pre-treatment of high strength food waste digestate by high content aluminum-nanocluster based magnetic coagulation

Tharindu Ritigala[1,2,4,**], *Hailu Demissie*[3,4,8,**], *Yanlin Chen*[1,2], *Jiaxi Zheng*[1,2], *Libing Zheng*[1,2], *Jinxing Zhu*[5], *Hua Fan*[5], *Jiao Li*[5], *Dongsheng Wang*[3,4], *Sujithra K. Weragoda*[6], *Rohan Weerasooriya*[7], *Yuansong Wei*[1,2,4,7,*]

[1] *State Key Joint Laboratory of Environmental Simulation and Pollution Control, Research Center for Eco-Environmental Sciences, Chinese Academy of Sciences, Beijing 100085, China*
[2] *Laboratory of Water Pollution Control Technology, Research Center for Eco-Environmental Sciences, Chinese Academy of Sciences, Beijing 100085, China*
[3] *State Key Laboratory of Environmental Aquatic Chemistry, Research Center for Eco-Environmental Sciences, Chinese Academy of Sciences, Beijing 100085, China*
[4] *University of Chinese Academy of Sciences, Beijing 100049, China*
[5] *Beijing Environmental Engineering Technology Co., Ltd, Beijing 100101, China*
[6] *National Water Supply and Drainage Board, Katugastota 20800, Sri Lanka*
[7] *National Institute of Fundamental Studies, Hantana Road, Kandy 20000, Sri Lanka*
[8] *Department of Chemistry College of Natural Sciences, Arbaminch University 1000, Ethiopia*

ARTICLE INFO

Article history:
Received 16 October 2020
Revised 7 December 2020
Accepted 22 December 2020
Available online 4 January 2021

Keywords:
Magnetic coagulation
Keggin nanocluster
Pre-treatment
Removal mechanism
Cost analysis

ABSTRACT

Coagulation-based pre-treatment efficiency of high strength digestate of food waste (HSDFW) anaerobic digestion is negated by organic ligand-catalyzed decomposition of coagulants. In this study, an efficient HSDFW pre-treatment method, magnetic seeds (MS) coagulation, was employed by using highly stable Keggin Al_{30} nanocluster (PAC_{30}), MS and polyacrylamide (PAM), and its operation was optimized by evaluating the performance of removing turbidity, total suspended solids (TSS), chemical oxygen demand (COD), and total phosphorous (TP) phosphate. Results showed that at the optimum dosage of 4.82 g/L, PAC_{30} demonstrated excellent removals as high as 98.93% ± 0.1% of turbidity, 98.04% ± 0.1% of TSS, 58.28% ± 0.3% of total COD, 99.98% ± 0.01% of TP and 99.50% ± 0.01% of dissolved phosphate, respectively. Apparent molecular weight (AMW) and three-dimensional excitation-emission matrix (3D-EEM) fluorescence spectroscopy analyses demonstrated more efficient removal of dissolved organic matter (DOM), particularly non-biodegradable and hydrophobic compo-

* Corresponding author.
E-mail: yswei@rcees.ac.cn (Y. Wei).
** Both the authors contributed equally to this article.

https://doi.org/10.1016/j.jes.2020.12.027

nents by PAC_{30} than commercial coagulant. The sedimentation was much improved from 40 min by coagulation/flocculation to about 5 min settling by MS coagulation. The PAC_{30} based magnetic coagulation (MC) presents theoretical guidance on a cost-effective and much less footprint pre-treatment alternative for high strength wastewater.

Introduction

Food waste (FW) is one of the largest category of municipal solid waste (MSW) disposed by landfill in the United States, accounting for approximately 18% of the waste stream. The FW is found to be three times methane production potential (376 m^3 gas/ton) compared with biosolids (120 m^3 gas/ton) (United States of Environmental Protection Agency, 2007). Consequently, anaerobic digestion (AD) pioneered as a well-established technology is employed worldwide to convert the organic fraction of municipal solid wastes as an auxiliary resource into methane gas, and that can be used to produce heat, electricity and vehicle fuel (Labatut and Pronto, 2018). The resulting effluent of the anaerobic digester known as digestate or digested liquor has been widely used as a fertilizer due to the presence of dozen useful nutrients (Lotti et al., 2019). However, the direct discharge of the digestate can cause possible environmental problems such as nitrate leaching, ammonia emissions into the atmosphere, and causing eutrophication (Nkoa, 2014). Thus, the digestate is claimed as remained non-friendly to the environment, as its obviously rich with a high concentration of direct pollution-causing spectrum components. Along with more and more stringent recent environmental standards, its treatment before discharge becomes an urgent need.

Although the presence of highly concentrated soluble pollutants (Xia and Murphy, 2016) and complex chemical composition (Scaglione et al., 2017) makes the treatment of the liquid digestate more complicated, it is most commonly post-treated with the combination of physicochemical methods (e.g., ammonia stripping) (Törnwall et al., 2017) and conventional biological treatment processes. In contrast, the digestate treatment cost was recognized as the main constraint for spreading AD technology (Lotti et al., 2019; Xia and Murphy, 2016). The use of enhanced biological methods is supposed to reduce these costs, and cost-effective biological treatment processes have been developed for the liquid digestate treatment, such as deammonification process (Chini et al., 2019), aerobic granular sludge process (Świątczak et al., 2019), partial nitritation (PN), anammox process (Lotti et al., 2019) and anaerobic fixed-film process (Demirer et al., 2019). However, the effectiveness of the biological processes for the liquid phase treatment is hampered by the high concentration of pollutants in the digestate, such as ammonium (Lotti et al., 2019), chemical oxygen demand (COD), total suspended solids (TSS) (Świątczak et al., 2019), free ammonia (Liu et al., 2019), conductivity, temperature (Wang et al., 2019), phosphate, sulfate and heavy metals (Feng et al., 2017), because the microorganism community and activity are sensitive to these factors. Hence, employing a cost-effective pre-treatment (to minimize excess pollutant load and remove suspended solids) is of great concern for the biological treatment of FW digestate in practice.

Generally, the physicochemical pre-treatment processes have been developed and applied in the wastewater treatment industry to improve the efficiency and performance of subsequent biological treatment processes and reduce microbial toxicity as well as operating costs (Ghimire and Wang, 2020). Coagulation/flocculation is widely used as a pre-treatment process for the treatment of domestic and industrial wastewater (Choumane et al., 2017), such as petrochemical hydrocarbon wastewater (Ribera-Pi et al., 2020), lead (Pb) smelting wastewater (Meng et al., 2020), saline industrial wastewater contaminated by hydrocarbons (Bruno et al., 2020), high strength olive processing wastewater (Esteves et al., 2019; Ozbey-Unal et al., 2018), dairy wastewater (Triques et al., 2020), landfill leachate (Luo et al., 2020) and vegetable oil refinery wastewater (Khouni et al., 2020).

Poly aluminum chloride (PAC) based coagulation is considered as the most popular coagulation, where its efficiency depends mainly on the polycation (Al_{13}) content, dosage, and characteristics of the wastewater (Matilainen et al., 2010). However, the presence of a small amount of Al_{13} in the commercial PAC coagulant and its instability in DOM's presence (Abeysinghe et al., 2013) is an insurmountable problem in the removal of dissolved organic matter.

Polynuclear aluminum nanocluster, $Al_{30}O_8(OH)_{56}(H_2O)_{24}^{18+}$ (Al_{30}), is another promising Gemini polycation with two δAl_{13} connected by four Al monomers and 2 nm in size (Fig. 1), which is less sensitive to pH fluctuation and more tolerable for temperature change (Allouche et al., 2000). Al_{30} achieves better turbidity removal than Al_{13} due to its higher sorption-neutralization nature, excellent sweep-flocculation, bridge-aggregation, and precipitation in the coagulation process by making use of its large-sized and high positive charge (Chen et al., 2006). It is also more resistant to DOM-ligand catalyzed decomposition than other species (Abeysinghe et al., 2013; Kimura et al., 2013). Inspired by the turbidity removal efficiency and structural composition, the polycation solution with a high content of Al_{30} was synthesized and employed for the treatment, where the application of this material for the treatment of high strength digestate is very scarce in the literature. Recently, the introduction of magnetic nanoparticles and polyelectrolyte into the coagulation process has attracted attention in enhancing performance (Kimura et al., 2013; Zhang et al., 2017; Zheng et al., 2020). Since the high ionic density and other related characteristics of FW decelerates the sedimentation rate in the conventional coagulation process, magnetic seed and polyelectrolyte are supposed to play an important role in improving the floc structure and strength. MC has been used to treat municipal, oily and coal

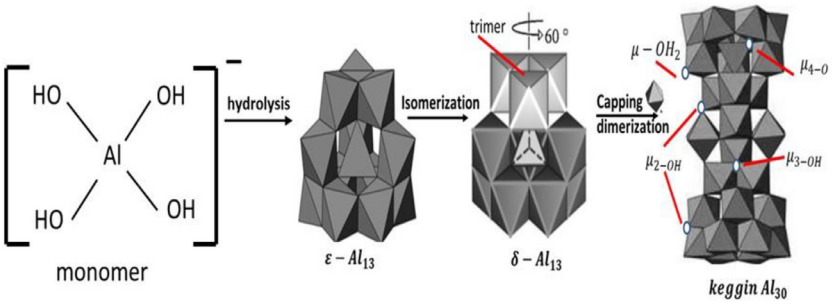

Fig. 1 – Schematic of Al_{13} isomerization, thermal treatment and dimerization for Al_{30} synthesis.

wastewater, and has been found to perform better suspension removal than conventional coagulation due to quick, large and dense floc formation, with more than 80% TSS removal efficiency (Cao et al., 2017). Furthermore, MS can be recycled and reused (Zhang et al., 2016). Thus, the solid-liquid separation efficiency would be enhanced (Zhang et al., 2017), and resulting in shortening the treatment time and reducing the capital costs related to land use and reactor construction.

The main objective of this study was to optimize a high content Keggin Al_{30} nanocluster (PAC_{30}) based MC pretreatment, in such a way to tackle the above bottlenecks of the subsequent biological processes. MS and PAM were used, and their effect on the kinetics and fate of the process was investigated. The removal assay of DOM was investigated from AMW and 3D-EEM analyses. The process variables, such as pH, PAC_{30}, PAM, MS dosage and stirring speed, were also optimized through evaluating removal efficiencies of turbidity, TSS, COD, TP and phosphate. Besides, this study with the specific emphasis on settling time and chemical cost analysis may provide an insight into cost-effective magnetic coagulation pretreatment alternatives of FW digestates.

1. Materials and methods

1.1. *Wastewater characteristics*

The high strength FW digestate was collected from an anaerobically digested municipal food waste digester at Dongcun Biogas Company, Beijing, China, with the maximum daily digestate discharge capacity of 1000 m^3/day. The liquid phase of the digestate was taken after the mechanical dewatering process and filtered using 0.9 mm (Ø 200 mm * 50 mm, GB/T60031-2012) mesh size to remove the coarse particles. The characteristics of the FW digestate were listed in Appendix A **Table S1**.

1.2. *Preparation of aluminum nanocluster*

Fig. 1 describes the scheme of coagulant synthesis. The detail of coagulant synthesis and the product species characterization is available in Appendix A **Table S2**.

1.3. *Jar test procedures*

Standard jar tests were carried out by using a programed jar test apparatus consisting of 500 mL beakers and a six-paddle gang stirrer (MY3000-6N, Meiyu, China). The raw digestate sample was prepared by homogenizing the source water for 30 min. The pH of the samples was adjusted with 0.5 mol/L HCl and NaOH before pipetting a predetermined amount of MS, coagulant and PAM in the final 400 mL solution. The dosing and mixing procedures are briefly described in Appendix A **Table S3**. After quiescent settlement, the supernatant solution was withdrawn for residual turbidity (RT) measurement (2100Q Turbidimeter, HACH, USA). The concentrations of ammonium, COD, phosphate, and phosphorus in the supernatant were determined from the portion of the supernatant sample and compared with the raw water concentration. The samples were taken with a syringe before settlement for zeta potential measurement (pre-experiment).

1.4. *Analytical methods*

Dissolved components were analyzed after passing the supernatant samples through a 0.45 μm membrane filter. The standard method (APHA, 2017) was employed to analyze all the components except COD. The COD was determined by COD prefabricated tube reagent (HR 20-1500 mg/L, HACH, USA) using a HACH DR2800 (HACH, USA), whereas, concentrations of PO_4^{3-} -P, NH_4^+-N and total phosphorus (TP) were determined by spectrophotometry methods with dual-beam ultraviolet spectroscopy (TU-1901, Beijing General Instrument Co. Ltd, China). Ammonium molybdate and ascorbic acid solution were used as a reagent for diluted supernatant content of PO_4^{3-} before absorbance measurement. Ammonium molybdate and ascorbic acid solution were used for TP quantification after autoclaving the samples containing potassium thiosulphate. Nessler reagent (HJ 535-2009) was applied to quantify NH_4^+-N. Before mixing the reagents, all samples were diluted to the appropriate concentration from the samples obtained directly at the point of 3 cm under the liquid top layer of the jar. Ultra-pure water prepared by the Milli-Q water purification system (Millipore, China) was used for all solution preparation and dilution procedures. The sediments dried at 55 Pa and -50°C for 48 hr by the vacuum freeze drier were used to characterize the surface morphology of floc obtain with and without magnetic seed as well as a polyelectrolyte. The analysis was carried out by SEM (Quattro C, Thermo scientific, USA).

Apparent molecular weight (AMW) distributions analysis was carried out by a size exclusion chromatography analysis with a high-performance liquid chromatography (HPLC) system equipped with dual λ absorbance detector (Waters

2487, USA) and binary HPLC pump (BREEZ 1525, Waters, USA) at UV_{254} at room temperature. A TSK gel column (G3000 SW, C-No. SW 3600482) conditioned with 0.015 mol/L phosphate buffer solution (0.00255 mol/L NaH_2PO4, 0.00245 mol/L Na_2HPO_4, and 0.01 mol/L NaCl at pH 6.8) as the mobile phase before sample analysis. Three-dimensional excitation-emission matrix (3D-EEM) fluorescence spectroscopy was obtained using a fluorescence spectrophotometer (F-4600 FL, HITACHI, Japan). Floc particle size distribution was measured using a particle size analyzer (Mastersizer 2000, Malvern, UK).

In addition, several fluorescence indexes were calculated to determine the hydrophobicity and humification property of the dissolved organic components as follows:

Fluorescence index (FI) is determined as the ratio of emission intensity at 450/500 nm measured at an excitation wavelength of 370 nm (Eq. (1)).

$$FI = \frac{I_{Em450}}{I_{Em500}},\ \text{at Ex} = 370\ \text{nm} \quad (1)$$

Humification index (HIX) is determined as the ratio of fluorescence intensities for two integrated regions of the emissions scans: Em 435–480 nm divided by Em 300–345 nm, at Ex 254 nm (Eq. (2)).

$$HIX = \frac{\sum I_{Em\ 435-480}}{\sum I_{Em\ 300-480}},\ \text{at Ex} = 254\ \text{nm} \quad (2)$$

Biological index (BIX) is calculated at Ex 310 nm, by dividing the fluorescence intensity at Em 380 nm by that at Em 430 nm (Eq. (3)).

$$BIX = \frac{I_{Em380}}{I_{Em430}},\ \text{at Ex} = 310\ \text{nm} \quad (3)$$

2. Results and discussion

2.1. *Optimization of the magnetic coagulation process*

There has been studied that the commercial coagulants have been used for pre-treatment of surface and wastewater before the subsequent biological treatment processes (Zhang et al., 2017). Despite, they are thought to have an insurmountable problem in removing dissolved organic matter (DOM) from a water sample due to their cation-organic complex formation and decomposition by ligand catalyzed reaction. However, the current high basicity coagulant with more content of non-simplex polycationic nanocluster expected to be more resistant to form a dissolved complex and decomposition (Abeysinghe et al., 2013; Kimura et al., 2013), thereby settle down organic components and their colloids from the bulk of the digested sample, by taking in to account its unique destabilization properties for suspended solids (Chen et al., 2006).

2.1.1. *Effect of PAC_{30} dosage*

The species distribution of prepared PAC_{30} was described in Appendix A **Table S2**. Turbidity and COD were taken as the primary indicators during the optimization process throughout the study. Preliminary experiments were performed to identify the working pH range of PAC_{30} by taking the same dosage as the commercial PAC dosage that we use in our laboratory for pre-treatment of the same wastewater. The range of (2.4 – 5.5 g/L) PAC_{30} was added into 400 mL digestate sample solution and tested against a pre-adjusted sample pH (6.5 – 8.5) in the presence of 12.5 mg/L of PAM and 2.5 g/L of MS, arbitrarily used on the basis of literature (Cao et al., 2017; Chen et al., 2018). Accordingly, the sample with pH 8.0 clearly showed significant removals of turbidity and COD, most likely related to the efficient hydrolysis performance of polynuclear species (Chen et al., 2006) and ionization characteristics of organic component's functional group. Therefore, pH 8.0 was chosen in this study for the optimization of the remaining parameters. The experimental sequence was designed in the following successive ways: as a coagulant (PAC_{30}), flocculant (PAM), magnetic seeds (MS) optimization, finally, the optimum pH was investigated once again.

Fig. 2**a** stipulates the removal efficiencies of COD and turbidity against the various dosages of PAC_{30}. The COD and turbidity removal increased with dosage and eventually became the most significant at the dosage of 4.82 g/L owing to sufficient enmeshment and destabilization with the rise in coagulant components. Due to more vital attractive forces between PAC_{30} particles at high dosage, a floc with more robust resistance to shear stress was formed, which effectively destabilized suspensions. However, upon increasing coagulant dosages, the removal decreased once again. It should be related to the restabilization of suspension in the bulk media by the excess coagulant species (charge reversal). Besides, flocs cleavage into several pieces of a size similar to parent flocs is inferred at a very high dosage by large-scale fragmentation (Jarvis et al., 2005), which has a determinantal effect on the removal efficiency.

2.1.2. *Effect of PAM*

The inorganic salt-based coagulation treatment of HSDFW is thought to be improved using combination with suitable polymer flocculant aids. To investigate this effect, PAM (5 mg/L – 11.25 mg/L)) and an arbitrary amount of MS was introduced to the raw digestate sample during coagulation as per the procedure described in Appendix A **Table S3**. As presented in Fig. 2**b**, the turbidity and COD removals were slightly increased with increasing PAM dosage and reached a maximum. It can be explained in terms of sweep flocculation, electrostatic patch and polymer flocculant bridging (Bolto and Gregory, 2007; Sun et al., 2020). Despite, after a certain range of dosage, the removals of COD and turbidity started to decrease again due to the presence of excess polymer and trace of turbidity-causing components in bulk adhered to it in bulk. The maximum COD removal (51.04%), and turbidity removal (99.39%) were achieved at 8.75 mg/L of PAM dosage. The maximum turbidity removal, 99.52%, was achieved at PAM dosage of 11.25 mg/L, which had a negligible difference with that of using 8.75 mg/L dosage. Strangely the COD removed at this dosage (41.27%) was found below the pre-planned removal efficiency and was nearly achievable with commercial PAC products (Table 1) (Wan et al., 2011). Hence, the polymer dosage at 8.75 mg/L was concluded as the optimum dose by taking into consideration COD removal as the most important issue and employed for the rest of the experiments in this study.

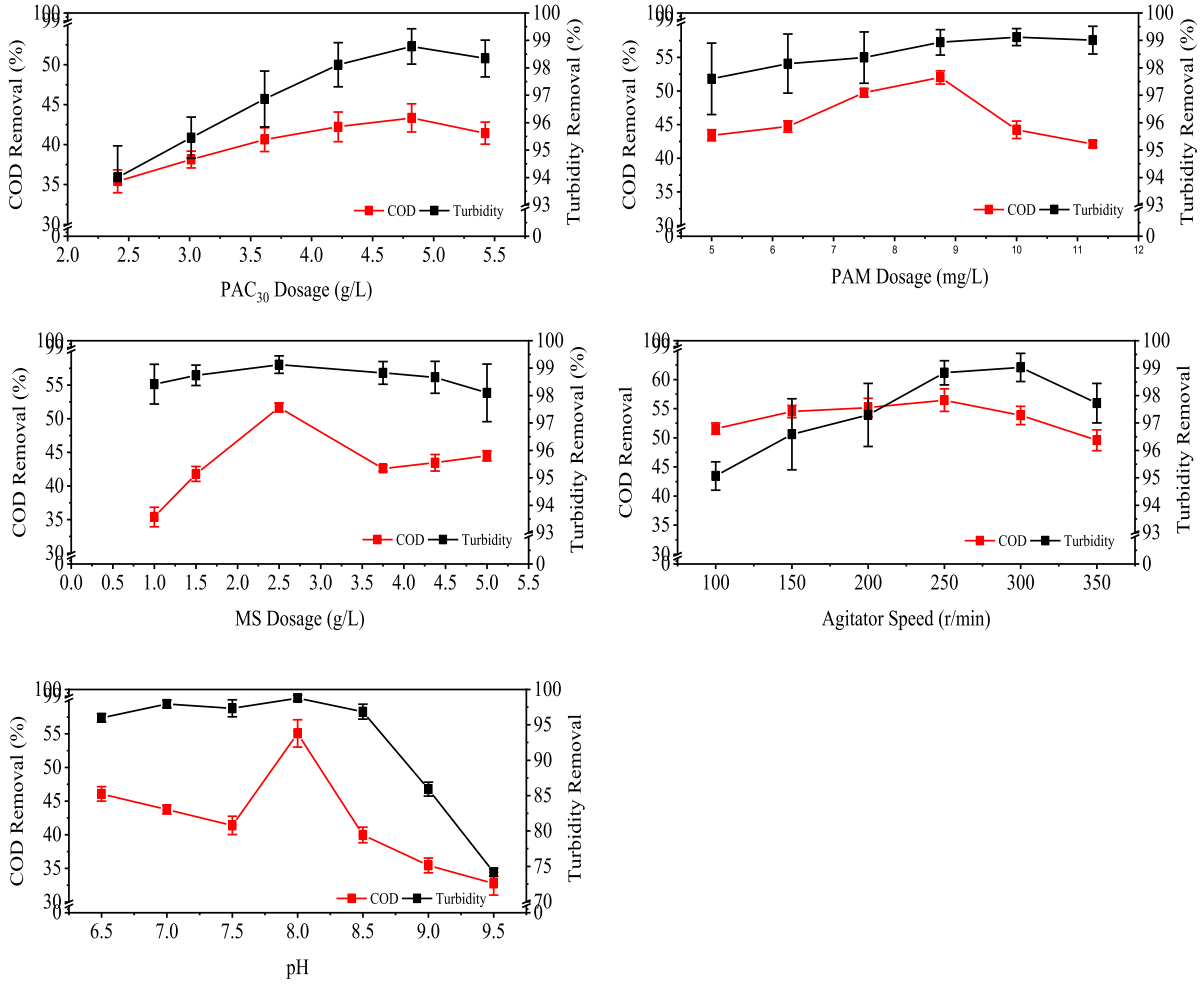

Fig. 2 – (a) Effect of PAC_{30}:12.5 mg/L PAM and 2.5 g/L MS, (b) effect of PAM: 4.82 g/L of PAC_{30}), (c) effect of MS: 4.82 g/L PAC_{30}, 8.75 mg/L of PAM, (d) effect of pH: 4.82 g/L PAC_{30}, 8.75 mg/L PAM, 2.5 g/L of MS, and (e) effect of Stirring Speed: 4.82 g/L PAC_{30}, 8.75 mg/L PAM, 2.5 g/L of MS on COD and turbidity removal with respective pH of 8.

2.1.3. *Effect of MS dosage*

Since the high ionic strength of the coagulation media (FW digestate) suppresses the settling rate of the coagulum, the process needs to be supplemented by additives, like MS. Where coagulant, MS and target pollutants coagulate together, and the resulting "seed-coagulant-pollutant" agglomerates are subsequently removed from the suspension either by sedimentation or filtration.

The effect of magnetic (Fe_3O_4, the average particle size of 280-300 mesh) was studied by increasing the dosage from 2.5 to 6.25 g/L (Fig. 2**c**) in a coagulation media. The maximum turbidity removal (99.39%) was achieved at 2.5 g/L of seed combined with optimum PAC_{30} and PAM dosage. The removal was then slightly decreased with increasing dosage, as the excess seed enhances the formation of more crystalline floc with less sorbing/enmeshment potential; it may incline to settle the coagulum before the completion of the proper coagulation process (Section 3.3). Likewise, the maximum COD removal (50.96%) was achieved at about 2.5 g/L of MS dosage and gradually decreased with increasing its dosage.

2.1.4. *Effect of pH*

The pH of raw water is the other process variable having an important effect on the removal of pollutants (suspended and other related components) as it can alter both hydrolysis characteristics and the binding site of the coagulant as well as the nature of the contaminant (Chen et al., 2006).

During the preliminary experiment, the optimum pH value was determined in the absence of PAM and MS and nonoptimized PAC_{30} dosage. The influence of pH value, particularly on turbidity and COD removals, was determined by a varying range of raw FW digestate pH values (6.5 – 9.5) with an optimized coagulant, PAM, and MS dosages. As shown in Fig. 2**d**, the pH was 8.0, corresponding to the minimum residual turbidity and COD value with the removals of 99.40% and 51.15% of turbidity and COD, respectively. The increase in removal efficiency with pH was attributed on the one hand, via the increase in the negative nature of the colloidal suspension, which can bind effectively with high positively charged coagulant aggregate by turn with MS and PAM, on the other hand via improving the partial hydrolysis characteristics of polynu-

Table 1 – Summary of removal efficiency under optimized condition after 30 minutes of settling.

Coagulation Steps	Turbidity Removal (%)	TSS Removal (%)	COD Removal (%)			TP Removal (%)			Nutrient Removal (%)	
			tCOD	sCOD	pCOD	TP_{total}	$TP_{soluble}$	$TP_{suspended}$	PO_4^{3-}	NH_4^+
PAC_{30}	96.89 ± 0.1	86.93 ± 0.1	54.44 ± 0.3	38.62 ± 0.4	90.53 ± 0.1	97.88 ± 0.3	99.03 ± 0.01	87.93 ± 0.01	99.19 ± 0.01	19.67 ± 0.01
PAC_{30}+PAM	98.82 ± 0.1	98.69 ± 0.1	56.80 ± 0.3	40.85 ± 0.4	93.20 ± 0.1	98.60 ± 0.3	99.89 ± 0.01	87.44 ± 0.01	99.39 ± 0.01	20.37 ± 0.01
PAC_{30}+PAM+MS	98.93 ± 0.1	98.04 ± 0.1	58.28 ± 0.3	41.60 ± 0.4	96.36 ± 0.1	98.79 ± 0.3	99.98 ± 0.01	88.51 ± 0.01	99.50 ± 0.01	20.20 ± 0.01
Commercial PAC+PAM+MS	95.10 ± 0.1	92.21 ± 0.1	33.64 ± 0.3	11.18 ± 0.4	88.44 ± 0.1	95.15 ± 0.3	97.31± 0.01	84.64 ± 0.01	90.03 ± 0.01	13.28 ± 0.01

tCOD:total chemical oxygen demand; sCOD: dissolve/soluble oxygen demand; pCOD: particulate/suspended oxygen demand; TP_{total}: total phosporus; $TP_{soluble}$: soluble phosphorus; $TP_{suspended}$: suspended phosphorus

clear coagulant (Chen et al., 2006). Although the partial hydrolysis of polycationic species increases at a very high pH value, the hydrolysis products' positive charge may be gradually reduced, and the electro-neutralization would decline, which resulted in the increase of the residual turbidity (COD). Besides, the other species $Al(OH)_4^-$ or $Al(OH)_3$ were expected to be formed, and turbidity and COD removal was thus decreased due to changes in removal mechanism and sorption efficiency in addition to charge reversal (Chen et al., 2006).

2.1.5. *Effect of stirring speed*

To investigate the effect of stirring speed on the treatment of FW digestate, the experiment was carried out in the range of stirring speed (100 r/min – 350 r/min) with optimum conditions of pH, PAC_{30}, PAM, and MS (**Fig. 2e**). The residual turbidity and COD were gradually decreased by increasing stirring speed. The maximum removals of turbidity at 99.40% and COD at 52.88% were attained at 300 r/min and 250 r/min, respectively. The turbidity and COD removals were decreased slightly at a stirring speed of 350 r/min. Except for the discrepancy in the removal between COD and turbidity at 300 r/min, the cause seems reasonably related to the strong kinetic energy and hydraulic shear. The shear force disperses the flocs and kinetic energy, which leads to floc's breakage. Since the turbidity removal at 250 r/min was 99.40%, which had an insignificant difference with the removal at 300 r/min, 250 r/min of the stirring speed was thus chosen as the optimum speed in this study. The velocity gradient (G) is a very important factor when it comes to determining the probability of the particles coming together. As a result, the G value was calculated according to (Jarvis et al., 2005) (Supporting Information). The velocity gradient value of 522.23 sec^{-1} and 48 sec^{-1} for rapid and slow mixing were respectively, achieved in this study. It appears that the G value of 500 sec^{-1} - 600 sec^{-1} (250 r/min - 300 r/min) and 48 sec^{-1} -75 sec^{-1} (50 r/min - 70 r/min) are the most favorable gradient of rapid and slow mixing, which are in agreement with the standard limit. The excessive velocity gradient causes floc rupture, while excessive time allows flocs erosion to occur (Mhaisalkar et al., 1986; Mohammed and Shakir, 2018).

The flocculation stage mainly causes the effective collision between small flocs (Ma et al., 2016) and agglomerate them into sediments. If the mixing intensity is too large, it will cause the particles to grow too fast and weaken the strength of the flower, by turn reduce removal efficiency. If the mixing intensity is too small, the probability of collision between small particles and large particles is drastically reduced, and small particles that are not flocculated are eventually ignored to be trapped by the settling coagulum (Sun et al., 2019).

2.2. *Nutrient removal*

Nitrogen and phosphorus are the main causes for eutrophication, and eventually leading to aquatic environmental deterioration (Boeykens et al., 2017). Since the FW digestate is known to contain a high concentration (Appendix A Table S2) of ammonia nitrogen and phosphorous (Zuriaga-Agustí et al., 2016), they need to be controlled or efficiently removed before the subsequent biological process in order to meet the discharge standards.

2.2.1. *Phosphorus removal*

The change in phosphate removal during coagulation with various dosages of PAC_{30}, PAM, MS and pH is presented in Appendix A **Fig. S1**. The pH corresponding to the maximum removal of phosphate was 7.0, different from that of both COD and turbidity removals discussed above. Although there exists a marked discrepancy in the removal trend of phosphate, turbidity, and COD with pH variation, the observed removal of phosphate was 98% at pH 8.0. However, this removal is sufficient enough compared with other coagulants' performance (Table 1). Hence, pH 8.0 was chosen as it offered the optimum removal of both turbidity and COD (Section 3.1.4), and the residual phosphate would be easily degraded by the subsequent process. As pH increased and eventually (>9.0), the positive surface charge of the floc/coagulant particle decreases, and other Al species appear, which consequently suppress the removal. Although the positive surface charge is very high at lower pH value (≤6), the polycation suffers from hydrolysis/flocculation; hence the phosphate removal was negligible (confirmed during pre-experiment).

The effect of PAC_{30} on the removal of phosphate was monitored at a fixed initial pH of the FW digestate. Accordingly, phosphate removal appeared to increase with the rise in PAC_{30} dosage, suggesting electrostatic/binding site increase with increased particles/floc fraction. In addition, shear resistant flocs formed due to high PAC_{30} dosage can effectively bind the phosphate (Jarvis et al., 2005). The effect of both PAM and MS on particulate and dissolved phosphorus removal resembled their effect that was discussed above on the removal of other components. In general, these investigations prove the efficient removal of phosphate and reduction of COD simultaneously from FW; consequently, it would help to enhance the performance of subsequent biological treatment.

2.2.2. *Ammonia nitrogen ($NH_4^+ - N$) removal*

Nitrogenous matter in wastewater can be divided into two categories: non-biodegradable and biodegradable. The non-biodegradable nitrogenous fraction is associated with the non-biodegradable particulate, chemical oxygen demand (COD).

Since the particulate fractions were effectively removed from digestate sample (Section 2.1.1), here, particular emphasis was given to the dissolved components, particularly $NH_4^+ - N$ removal. As listed in Appendix A **Table S1**, the ammonium content (1861 mg/L) was more than 75% of the total nitrogen (2244 mg/L) in the raw FW digestate. As shown in Appendix A **Fig. S2**, the removal of $NH_4^+ - N$ was improved with increasing the dosage of PAC_{30}, PAM, and MS, except for the pH change. Nearly 20% of removal was achieved at optimum condition. Although the removal of dissolved nitrogen was appeared not as significant as phosphorus removal, it was expected to be efficiently removed by the subsequent biological process.

2.3. *Removal efficiency of pollutants under optimized conditions*

2.3.1. *Suspended/Particulate contaminants*

It is apparent from Table 1 that turbidity removal with only PAC_{30} was 97%, attributed to sufficient destabilization of colloidal particles with a strong charge on nanocluster (Chen et al., 2006; Kimura et al., 2013). However, some fraction of very small flocs remaining suspended might be responsible for residual turbidity, but which were well collected by introducing PAM to the media; thus, turbidity and TSS removals were each increased to 99% in the presence of optimum PAM dosage. However, the MS introduction to the media was shown to have less effect on their removals, as it supplements the coagulation by predominantly improving the settling rate (Section 3.5). Concomitant with turbidity removal, the 54% removal of total COD (Table 1) was achieved by coagulation with PAC_{30} alone; the COD removal was increased to 57% by introducing PAM while no significant change was observed on the removal by adding MS. The removal of particulate COD (pCOD) was eventually increased to 96.36% in the presence of PAM, and MS spiked jar test samples. In contrast, both total phosphorus and phosphate removals were found to have negligible change after introducing both PAM and MS, except a relative improvement in particulate phosphate removal.

2.3.2. *Dissolved contaminants*

As shown in Table 1, about 38.62% and 90.53% of removal belonged to dissolved and particulate COD, respectively, related to the effectiveness of the high basicity coagulant on dissolved organic compounds removal (Abeysinghe et al., 2013; Kimura et al., 2013), which cannot be achieved with conventional coagulants (Appendix A **Table S4** and Fig. 3).

Fig. 3 shows that PAC_{30} achieved more removals of both low AMW and high AMW dissolved organic matter (DOM). Because the H_2O and OH^- found around the belt sphere of Al_{30} polycation (Fig. 1) which can exchange proton with a bulk media (Chen et al., 2006), and the deprotonated site can effectively bind with functional groups (ligands) of dissolved organics. Unlike the complex of simplex aluminum species, the resulting complex with the nanocluster product is insoluble in nature (Kimura et al., 2013), and then easily converts into amorphous flocculate, that still having a sorbing potential. Some dissolved organics can also directly bind to the reactive proton exchangeable site around the bridging unit of Al_{30} by completing the puerperal coordination and coagulate them to amorphous flocculates (Demissie et al., 2020). Although there has been increased floc size for all samples dosed with PAM (Fig. 4), the intensity of AMW spectra increased as compared to the same sample treated with coagulant alone or with MS (Fig. 3). This can be explained that a certain unbind fraction of PAM remained in the bulk after coagulation is related to the spectra. Not only large AMW but also small AMW spectral were changed, owing to the product of chemical reaction with the complex mixture of sample components. In general, almost in all cases, the removals of the dissolved component by PAC_{30} were not highly influenced by the presence of supplementary components, reflecting that they were mainly aiding the process.

3D EEM spectroscopy was applied to investigate the fate of DOM removal in the presence of PAC_{30} and commercial PAC with MS and further determine the degradation behaviour of pollutants in wastewater. Fig. 5**a** clearly shows the distinctive peaks at A (E_X/E_M=200-240 nm/275-330 nm), B (E_X/E_M=205-240 nm/330-380 nm) which belongs to sim-

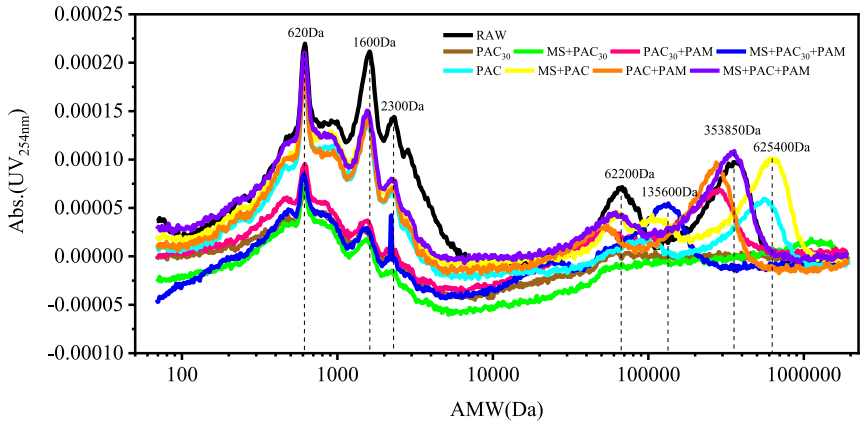

Fig. 3 – The apparent molecular weight (AMW) chromatogram of UV response at 254 nm for raw water and treated water by PAC_{30} and PAC in the absence or presence of coagulant aids at optimized conditions at pH=8.0 (For PAC_{30}, MS = 2.5 g/L, PAC_{30} = 4.82 g/L, PAM = 8.75 mg/L and Stirring speed = 250 r/min. For PAC MS = 3.0 g/L, PAC_{30} = 12.0 g/L, PAM = 12.5 mg/L and Stirring speed = 250 r/min).

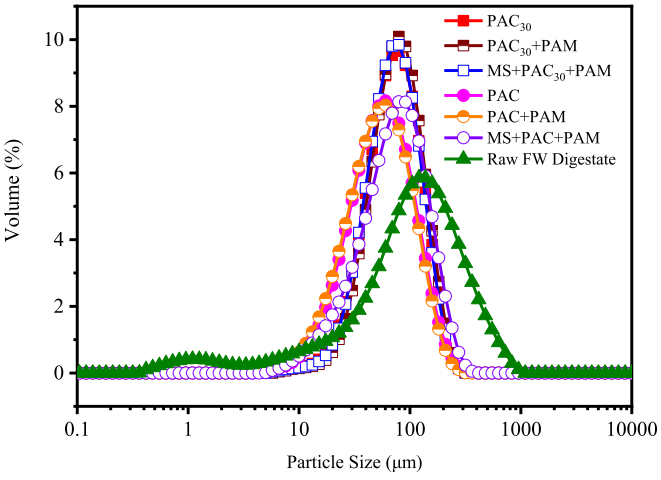

Fig. 4 – The mean particle size distribution of floc collected after coagulation with PAC30 and PAC coagulants at optimized conditions at pH=8.0 (For PAC_{30}, MS = 2.5 g/L, PAC_{30} = 4.82 g/L, PAM = 8.75 mg/L and Stirring speed = 250 r/min For PAC, MS = 3.0 g/L, PAC_{30} = 12.0 g/L, PAM = 12.5 mg/L and Stirring speed = 250 r/min).

ple aromatic proteins such as tyrosine-like and tryptophan-like substances, C (E_X/E_M=210-245 nm/380-425 nm) and D (E_X/E_M=240-270 nm/390-450 nm) respectively correspond to fulvic-like and humic-like substances, E (E_X/E_M=260-300 nm/270-380 nm) represents soluble microbial by product-like substances (Jia et al., 2014; Yu et al., 2020). Moreover, Fig. 5**b** and 5**c** show an intense peak at E_X/E_M 200-225 nm/275-325 nm correspond to hydrophobic neutrals (HON) (Leenheer and Croué, 2003). EEM spectra (Fig. 5**a**) exhibited the hydrophobic components than the hydrophilic component and experiment show PAC_{30} removed most of the hydrophobic less readily biodegradable or transformable substances e.g. external foulant, soluble microbial products and more extracellular polymeric like substances from the wastewater than PAC (Fig. 5**d** and 5**e**) (Xiao et al., 2019, 2016).

In addition to EEM spectra, fluorescence indices were calculated to determine the nature of DOM and its removal (Appendix A **Table S5**). The fluorescence index (FI) of FW digestate (FI=2.97) was higher than 1.9, which means that the DOM was mainly autochthonous derived (McKnight et al., 2001; Rodríguez-Vidal et al., 2020). Whereas the biological index (BIX) was 1.71, which is higher than 1, indicates a biological or aquatic bacterial origin of DOM (Zheng et al., 2020; Zsolnay et al., 1999). The humification index (HIX) of the FW digestate was 0.04 indicated in situ formation of DOM due to biological activities (Huguet et al., 2009; Rodríguez-Vidal et al., 2020; Zheng et al., 2018). Results confirmed that PAC_{30} based magnetic coagulation showed excellent DOM removal (FI =1.04, BIX = 0.93, HIX = 0.01) compared with commercial PAC (FI = 2.67, BIX = 1.20, HIX = 0.02).

2.3.3. *Particle size*

The particle size distribution of raw water and samples after coagulation (with different coagulants) was shown in Fig. 4. As shown in Fig. 3, the particle size of samples after coagulation with both PAC_{30} and PAC increased with spiking MS and further increased with PAM dosage. The most significant increase in size was observed in the case of PAC_{30}. A similar phenomenon was observed in the floc structure obtained from SEM analysis. Although the floc of PAC_{30} is assumed to have high sorbing potential due to high surface area, and smooth glossy (amorphous) surface (Appendix A **Fig. S3a**), its sedimentation rate was hampered by the high ionic density of the sample water. However, using coagulant aids, particularly, MS, is accompanied by the formation of sheer resistant and heavier flocs (Appendix A **Fig. S3b**). Moreover, PAM addition (Appendix A **Fig. S3c**) was found to enmesh formed flocs, which could thus significantly minimize the settling time (Section 3.5).

2.4. *Proposed mechanism of MS coagulation*

In summary, the removal model for DOM by MS and coagulants could be assumed as Fig. 6. There exist different pos-

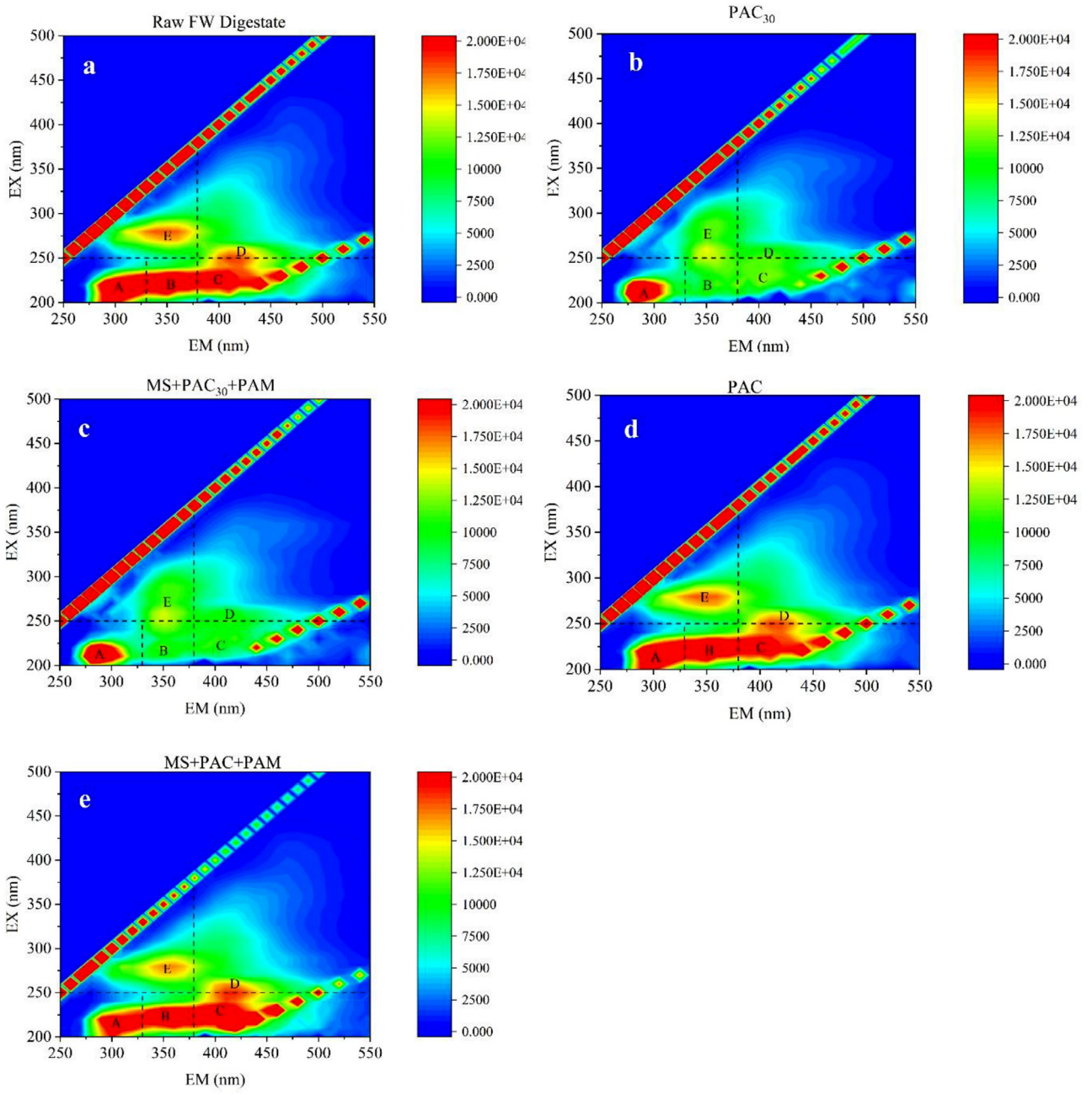

Fig. 5 – Excitation emission spectroscopy of (a) Raw FW digestate, (b) coagulation with PAC_{30}, (c) MS+PAC_{30}+PAM, (d) Commercial PAC, (e) MS+Commercial PAC+PAM: at optimum conditions, except (a).

sible mechanisms due to the complex behaviour of coagulant species in water, and the diversity of DOM. Among them, four typical floc states were formed due to the complicated chemical-physical process after coagulant injection. (1) MS introduction increases collision frequency and decreases the average distance between particles (Brownian motion), which lead to high sedimentation and turbidity removal due to high density; (2) Also, the complex matrix of MS and Al species can effectively destabilize suspended (colloidal) particles; (3) Fe-O-X of MS may interact either with coagulants or protonated/ deprotonated site of DOM via ligand exchange, hydrogen bonding and complexing reactions, thus flocculate together (Al_{30} in PAC_{30} might have more tendency than others due to its more proton exchangeable sites) (Abeysinghe et al., 2013). (4) MS can be used as a sorption substrate (nuclei) for coagulant species, particularly for polymeric species, by turn oppositely charged DOM binds effectively on the positively charged layer, and the final densely structure would flocculate readily (Zhang et al., 2017; Zhu et al., 2020). The negative zeta potential value of MS at working pH signifies this phenomenon. PAM is mostly known by more bridging these formed particles together.

2.5. *Settling time and chemical costs analysis*

The settling time during the coagulation process with commercial PAC and PAC_{30} in the presence and absence of MS was

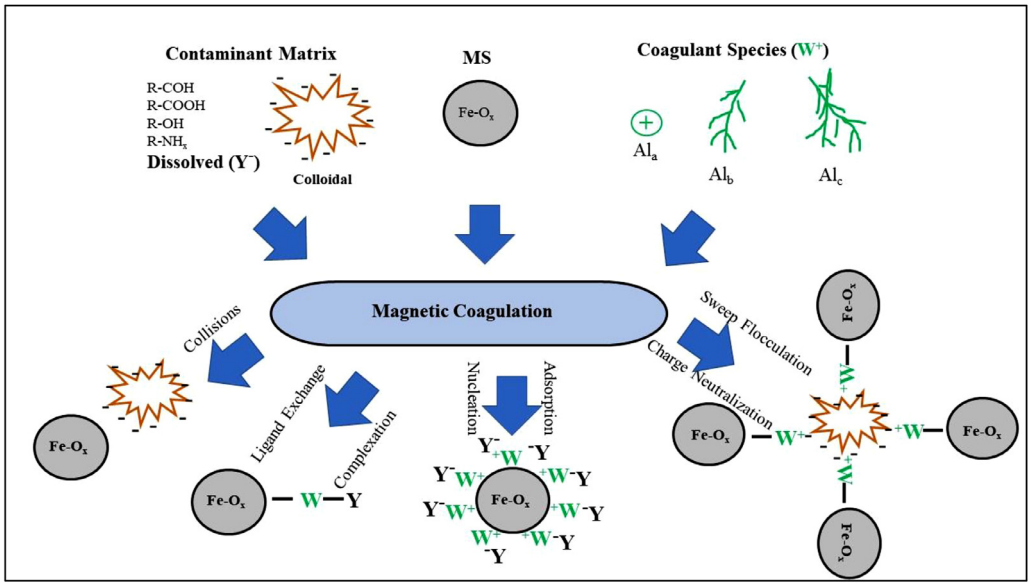

Fig. 6 – Mechanism of MS coagulation.

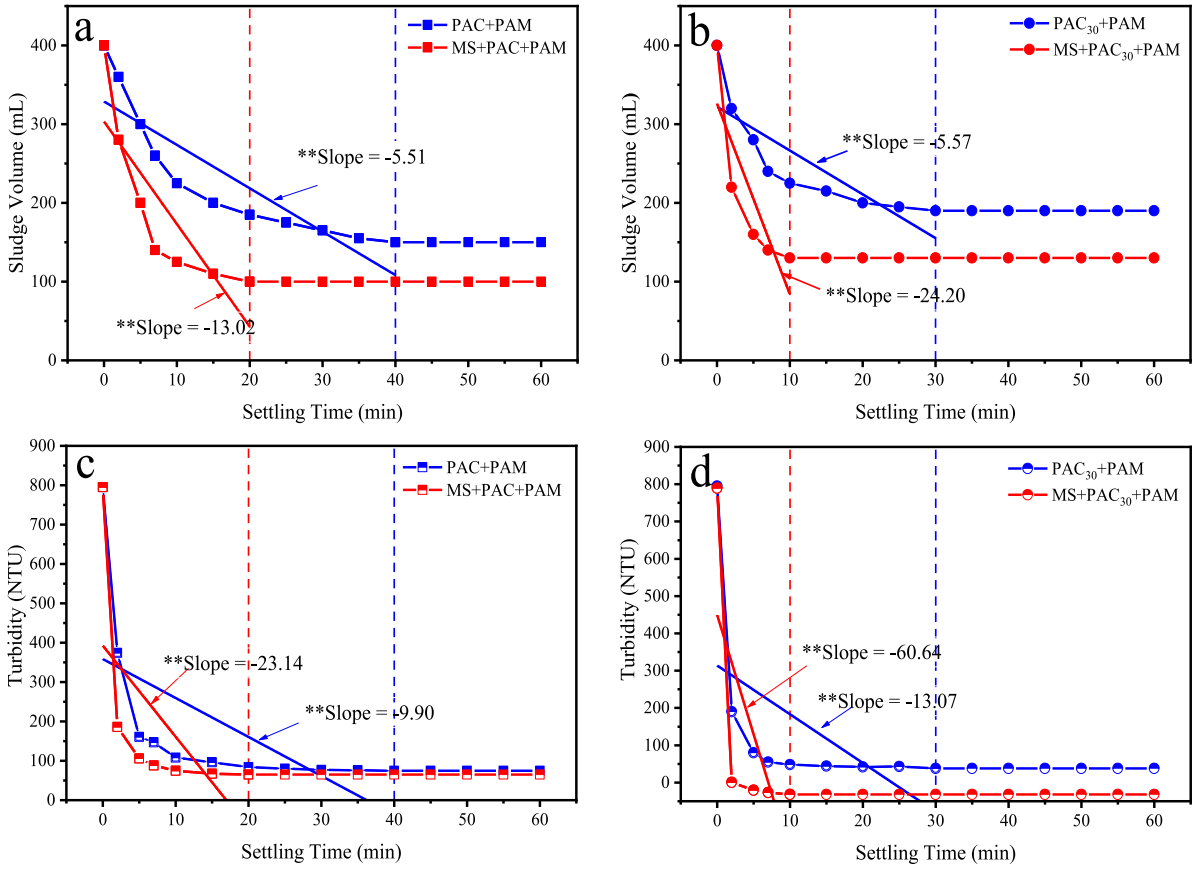

Fig. 7 – Effect of commercial PAC and PAC_{30} with presence and absence of MS sludge volume at different settling time, (a) PAC, (b) PAC_{30}, and turbidity value at different settling time (c) PAC, (d)PAC_{30}: at optimum conditions. The slope is considered upto inflation point. ** denoted 95% significant level.

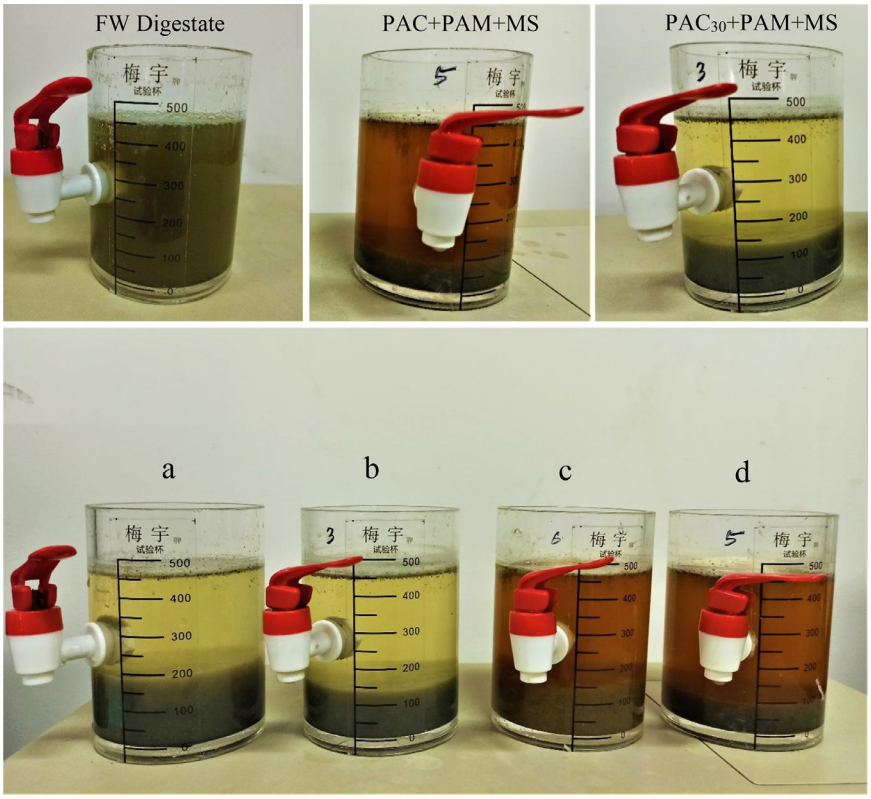

Fig. 8 – Coagulation experiment results with optimum dosages after 60 minutes settling time (a) PAC_{30}+PAM, (b) PAC_{30}+PAM+MS, (c) Commercial PAC+PAM, (d) Commercial PAC+PAM+MS: at optimum conditions.

investigated. Turbidity and corresponding sludge volume were observed with different settling times at optimum dosages of both coagulants (Appendix A **Table S6**). As shown in Fig. 7**b**, the turbidity removal was 98.06% and 92.68% for PAC_{30} and commercial PAC, respectively, after 5 min of magnetic coagulation. These values were nearly achieved without MS after 30 min, but the turbidity removal without MS after 5 min was only 94.48% and 88.88% for PAC_{30} and commercial PAC, respectively. The results clearly show MC is faster than conventional coagulation with both commercial PAC and PAC_{30}, with PAC_{30} showing higher turbidity removal. It, thus, can be deduced that the main function of the MS is to improve the settleability of floc.

As shown in Fig. 7**a**, less sludge volume is produced in coagulation with MS than with its absence, which was reduced by 31.58% and 33.33% for PAC_{30} and commercial PAC, respectively; and higher sludge compaction rate was observed in both coagulants combined with MS addition. The results show (Fig. 7**a**, 7**b**, and Fig. 8) the commercial PAC had a relatively low settling rate and less sludge volume than the PAC_{30} when employed in the absence and presence of MS. PAC_{30} was found to demonstrate not only a relatively faster settling rate but also was characterized by efficient removal of turbidity, COD, and other components (Fig. 8 **and** Table 1).

A combination of efficiency and cost-effectiveness is the essential prerequisites for the sustainable treatment process (Boguniewicz-Zablocka et al., 2019). Generally, the coagulation process's operating cost is related to the cost of energy, chemical, and sludge disposal (Yoo, 2018). A real case study needs to be carried out to conduct an accurate economic assessment. This study includes only the chemicals cost, which was carried out based on the available prices from 2020 given by the company (Xinying, Beijing, China); commercial chemical prices are presented in Appendix A **Table S7**. Since PAC_{30} is not yet commercialized, the emphasis was given for the PAC cost analysis, which can be cascaded for the PAC_{30} as its production process resembles the commercial products. The chemical cost was calculated from the optimum dosage, then the removal cost of 1kg of COD was estimated for each coagulation step (Fig. 9). The estimated chemical costs for the magnetic coagulation process under optimal conditions are 0.137 USD and 0.295 USD for PAC_{30} and commercial PAC, respectively, per cubic meter of the FW digestate.

Adding magnetic seeds to the coagulation process drastically accelerates the settling rate and reduces the settling tank volume. For instance, while the average settling time of conventional coagulation is 30 min (Marañón et al., 2008; Ren et al., 2019), the MC process settling time is approximately 5-7 min (Cao et al., 2017; Marañón et al., 2008). The settling time of MC was less than 5 min to reach 200 mL of sludge volume for the PAC_{30}+PAM+MS, which reduced the sedimentation tank volume tenfold, compared with 40 min of settling for that without MS (Fig. 7**a**). Even though the MC process was found to increase the chemical cost to some extent, it

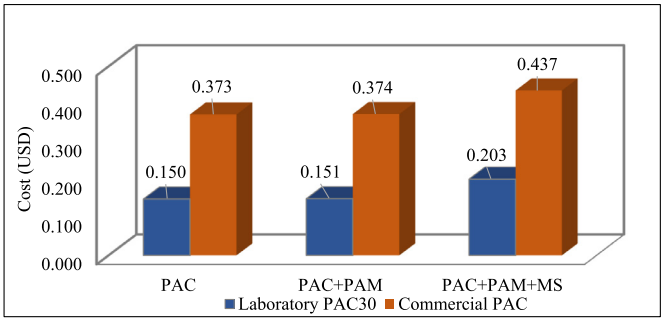

Fig. 9 – Comparison of chemical cost for each coagulation step to remove the 1kg of COD in FW digestate.

can be regarded as an important process in terms of saving the volume of the tank basins and improving the treatment capacity. In addition, the recovery of MS (approximately 99%) (Zhang et al., 2016) can further decrease the MS dosage and, consequently, the total chemical costs, which makes it a cost-effective alternative process in a limited space area and highly urbanized sites.

3. Conclusions

In this study, the high content of polynuclear nanocluster solution (PAC_{30}) was prepared as a coagulant and combined with MS for the pre-treatment of the FW digestate. Compared with commercial PAC, PAC_{30} was more effective in removing TSS (98.04% ± 0.1%), COD (58.28% ± 0.3%), TP (99.98% ± 0.1%) and phosphate (99.50% ± 0.01%). The optimized dosage of PAC_{30} was at 4.82 g/L, much less than that of commercial PAC. Results from AMW and 3D-EEM analysis showed that the small and large AMW molecules, and hydrophobic non-biodegradable dissolved components were most removed by PAC_{30}, which are the common bottlenecks for the subsequent biological process. The coagulation of PAC_{30} and MS shows a cost-effective method for the pre-treatment of FW digestate, because the MS speeds up the settling rate and drastically reduces settling time (40 to 5 min), saving many footprints for the coagulation- pre-treatment process of the FW digestate.

Acknowledgements

This work was supported by the National Key Research and Development Program of China (No. 2018YFD1100600); the Program of China-Sri Lanka Joint Center for Water Technology Research and Demonstration; China–Sri Lanka Joint Center for Education and Research by the Chinese Academy of Sciences; and the Chinese Government Scholarship Program (CSC No. 2018SLJ023250).

Appendix A Supplementary data

Supplementary material associated with this article can be found, in the online version, at doi:10.1016/j.jes.2020.12.027.

REFERENCES

Abeysinghe, S., Unruh, D.K., Forbes, T.Z., 2013. Surface modification of Al30 keggin-type polyaluminum molecular clusters. Inorg. Chem. 52, 5991–5999. doi:10.1021/ic400321k.

Allouche, L., Gérardin, C., Loiseau, T., Férey, G., Taulelle, F., 2000. Al30: a giant aluminum polycation. Angew. Chemie Int. Ed. 39, 511–514. doi:10.1002/(SICI)1521-3773(20000204)39:3⟨511::AID-ANIE511⟩3.0.CO;2-N.

APHA, 2017. Standard Methods for the Examination of Water and Wastewater, 23rd ed. American Public Health Association, Washington DC.

Boeykens, S.P., Piol, M.N., Samudio Legal, L., Saralegui, A.B., Vázquez, C., 2017. Eutrophication decrease: Phosphate adsorption processes in presence of nitrates. J. Environ. Manage. 203, 888–895. doi:10.1016/j.jenvman.2017.05.026.

Boguniewicz-Zablocka, J., Klosok-Bazan, I., Naddeo, V., Mozejko, C.A., 2019. Cost-effective removal of COD in the pre-treatment of wastewater from the paper industry. Water Sci. Technol. 1–9. doi:10.2166/wst.2019.328.

Bolto, B., Gregory, J., 2007. Organic polyelectrolytes in water treatment. Water Res. 41, 2301–2324. doi:10.1016/j.watres.2007.03.012.

Bruno, P., Campo, R., Giustra, M.G., De Marchis, M., Di Bella, G., 2020. Bench scale continuous coagulation-flocculation of saline industrial wastewater contaminated by hydrocarbons. J. Water Process Eng. 34, 101156. doi:10.1016/j.jwpe.2020.101156.

Cao, X., Mei, K., Li, X., 2017. Study on landfill leachate pretreatment by magnetic flocculation. Chinese J. Environ. Eng. 47, 956–962. doi:10.3969/j.issn.1001-0505.2017.05.019.

Chen, Y., Libing, Z., Chen, M., Wei, Y., 2018. Study on total phosphorus removal of swine wastewater with magnetic coagulation. Chin. J. Environ. Eng. 36, 154–159.

Chen, Z., Fan, B., Peng, X., Zhang, Z., Fan, J., Luan, Z., 2006. Evaluation of Al30 polynuclear species in polyaluminum solutions as coagulant for water treatment. Chemosphere 64, 912–918. doi:10.1016/j.chemosphere.2006.01.038.

Chini, A., Chiapetti, A., Ester, C., Goldschmidt, F., Fongaro, G., Treichel, H., Kunz, A., 2019. Evaluation of deammoni fi cation reactor performance and microrganisms community during treatment of digestate from swine sludge CSTR biodigester. J. Environ. Manage. 246, 19–26. doi:10.1016/j.jenvman.2019.05.113.

Choumane, F.Z., Benguella, B., Maachou, B., Saadi, N., 2017. Valorisation of a bioflocculant and hydroxyapatites as coagulation-flocculation adjuvants in wastewater treatment of the steppe in the wilaya of Saida (Algeria). Ecol. Eng. 107, 152–159. doi:10.1016/j.ecoleng.2017.07.013.

Demirer, N., Ülgüdür, N., Ergüder, T.H., Uluda, S., 2019. High-rate anaerobic treatment of digestate using fixed film reactors.

Environ. Pollut. 252, 1622–1632. doi:10.1016/j.envpol.2019.06.115.
Demissie, H., An, G., Jiao, R., Ritigala, T., Lu, S., Wang, D., 2020. Modification of high content nanocluster-based coagulation for rapid removal of dye from water and the mechanism. Sep. Purif. Technol., 117845 doi:10.1016/j.seppur.2020.117845.
Esteves, B.M., Rodrigues, C.S.D., Maldonado-Hódar, F.J., Madeira, L.M., 2019. Treatment of high-strength olive mill wastewater by combined Fenton-like oxidation and coagulation/flocculation. J. Environ. Chem. Eng. 7, 103252. doi:10.1016/j.jece.2019.103252.
Feng, Y., Lu, X., Al-Hazmi, H., Mąkinia, J., 2017. An overview of the strategies for the deammonification process start-up and recovery after accidental operational failures. Rev. Environ. Sci. Bio/Technol. 16, 541–568. doi:10.1007/s11157-017-9441-2.
Ghimire, N., Wang, S., 2020. Biological Treatment of Petrochemical Wastewater, in: Petroleum Chemicals - Recent Insight. https://doi.org/10.5772/intechopen.79655
Huguet, A., Vacher, L., Relexans, S., Saubusse, S., Froidefond, J.M., Parlanti, E., 2009. Properties of fluorescent dissolved organic matter in the Gironde Estuary. Org. Geochem. 40, 706–719. doi:10.1016/j.orggeochem.2009.03.002.
Jarvis, P., Jefferson, B., Gregory, J., Parsons, S.A., 2005. A review of floc strength and breakage. Water Res. 39, 3121–3137. doi:10.1016/j.watres.2005.05.022.
Jia, S., Han, H., Hou, B., Zhuang, H., Fang, F., Zhao, Q., 2014. Treatment of coal gasification wastewater by membrane bioreactor hybrid powdered activated carbon (MBR-PAC) system. Chemosphere 117, 753–759. doi:10.1016/j.chemosphere.2014.09.085.
Khouni, I., Louhichi, G., Ghrabi, A., Moulin, P., 2020. Efficiency of a coagulation/flocculation–membrane filtration hybrid process for the treatment of vegetable oil refinery wastewater for safe reuse and recovery. Process Saf. Environ. Prot. 135, 323–341. doi:10.1016/j.psep.2020.01.004.
Kimura, M., Matsui, Y., Kondo, K., Ishikawa, T.B., Matsushita, T., Shirasaki, N., 2013. Minimizing residual aluminum concentration in treated water by tailoring properties of polyaluminum coagulants. Water Res. 47, 2075–2084. doi:10.1016/j.watres.2013.01.037.
Labatut, R.A., Pronto, J.L., 2018. Chapter 4 - sustainable waste-to-energy technologies: anaerobic digestion. In: Trabold, T.A., Babbitt, W.B. (Eds.), Sustainable Food Waste-to-Energy Systems. Academic Press, pp. 47–67. doi:10.1016/B978-0-12-811157-4.00004-8.
Leenheer, J.A., Croué, J.P., 2003. Characterizing aquatic dissolved organic matter. Environ. Sci. Technol. 37. doi:10.1017/S0033822200003672.
Liu, Y., Ngo, H.H., Guo, W., Peng, L., Wang, D., Ni, B., 2019. The roles of free ammonia (FA) in biological wastewater treatment processes: a review. Environ. Int. 123, 10–19. doi:10.1016/j.envint.2018.11.039.
Lotti, T., Burzi, O., Scaglione, D., Ramos, C.A., Ficara, E., Pérez, J., Carrera, J., 2019. Two-stage granular sludge partial nitritation/anammox process for the treatment of digestate from the anaerobic digestion of the organic fraction of municipal solid waste. Waste Manag. 100, 36–44. doi:10.1016/j.wasman.2019.08.044.
Luo, H., Zeng, Y., Cheng, Y., He, D., Pan, X., 2020. Recent advances in municipal landfill leachate: A review focusing on its characteristics, treatment, and toxicity assessment. Sci. Total Environ. 703, 135468. doi:10.1016/j.scitotenv.2019.135468.
Ma, J., Fu, K., Shi, J., Sun, Y., Zhang, X., Ding, L., 2016. Ultraviolet-Assisted synthesis of polyacrylamide-grafted chitosan nanoparticles and flocculation performance. Carbohydr. Polym. 151, 565–575. doi:10.1016/j.carbpol.2016.06.002.
Marañón, E., Castrillón, L., Fernández-Nava, Y., Fernández-Méndez, A., Fernández-Sánchez, A., 2008. Coagulation–flocculation as a pretreatment process at a landfill leachate nitrification–denitrification plant. J. Hazard. Mater. 156bio, 538–544. doi:10.1016/j.jhazmat.2007.12.084.
Matilainen, A., Vepsäläinen, M., Sillanpää, M., 2010. Natural organic matter removal by coagulation during drinking water treatment: a review. Adv. Colloid Interface Sci. 159, 189–197. doi:10.1016/j.cis.2010.06.007.
McKnight, D.M., Boyer, E.W., Westerhoff, P.K., Doran, P.T., Kulbe, T., Andersen, D.T., 2001. Spectrofluorometric characterization of dissolved organic matter for indication of precursor organic material and aromaticity. Limnol. Ocean. 46, 38–48. doi:10.1016/j.scitotenv.2018.02.237.
Meng, X., Khoso, S.A., Jiang, F., Zhang, Y., Yue, T., Gao, J., et al., 2020. Removal of chemical oxygen demand and ammonia nitrogen from lead smelting wastewater with high salts content using electrochemical oxidation combined with coagulation–flocculation treatment. Sep. Purif. Technol. 235, 116233. doi:10.1016/j.seppur.2019.116233.
Mhaisalkar, V.A., Paramasivam, R., Bhole, A.G., 1986. An innovative technique for determining velocity gradient in coagulation-flocculation process. Water Res. 20, 1307–1314. doi:10.1016/0043-1354(86)90162-4.
Mohammed, T.J., Shakir, E., 2018. Effect of settling time, velocity gradient, and camp number on turbidity removal for oilfield produced water. Egypt. J. Pet. 27, 31–36. doi:10.1016/j.ejpe.2016.12.006.
Nkoa, R., 2014. Agricultural benefits and environmental risks of soil fertilization with anaerobic digestates: a review. Agron. Sustain. Dev. 34, 473–492. doi:10.1007/s13593-013-0196-z.
Ozbey-Unal, B., Balcik-Canbolat, C., Dizge, N., Keskinler, B., 2018. Treatability studies on optimizing coagulant type and dosage in combined coagulation/membrane processes for table olive processing wastewater. J. Water Process Eng. 26, 301–307. doi:10.1016/j.jwpe.2018.10.023.
Ren, X., Xu, X., Xiao, Y., Chen, W., Song, K., 2019. Effective removal by coagulation of contaminants in concentrated leachate from municipal solid waste incineration power plants. Sci. Total Environ. 685, 392–400. doi:10.1016/j.scitotenv.2019.05.392.
Ribera-Pi, J., Badia-Fabregat, M., Arias, D., Gómez, V., Taberna, E., Sanz, J., et al., 2020. Coagulation-flocculation and moving bed biofilm reactor as pre-treatment for water recycling in the petrochemical industry. Sci. Total Environ. 715, 136800. doi:10.1016/j.scitotenv.2020.136800.
Rodríguez-Vidal, F.J., García-Valverde, M., Ortega-Azabache, B., González-Martínez, Á., Bellido-Fernández, A., 2020. Characterization of urban and industrial wastewaters using excitation-emission matrix (EEM) fluorescence: Searching for specific fingerprints. J. Environ. Manage. 263. doi:10.1016/j.jenvman.2020.110396.
Scaglione, D., Lotti, T., Ficara, E., Malpei, F., 2017. Inhibition on anammox bacteria upon exposure to digestates from biogas plants treating the organic fraction of municipal solid waste and the role of conductivity. Waste Manag. 61, 213–219. doi:10.1016/j.wasman.2016.11.014.
Sun, Y., Sun, W., Shah, K.J., Chiang, P.-C., Zheng, H., 2019. Characterization and flocculation evaluation of a novel carboxylated chitosan modified flocculant by UV initiated polymerization. Carbohydr. Polym. 208, 213–220. doi:10.1016/j.carbpol.2018.12.064.
Sun, Y., Zhou, S., Chiang, P.-C., Shah, K.J., 2020. Evaluation and optimization of enhanced coagulation process: water and energy nexus. Water-Energy Nexus doi:10.1016/J.WEN.2020.01.001.
Świątczak, P., Cydzik-Kwiatkowska, A., Zielińska, M., 2019. Treatment of the liquid phase of digestate from a biogas plant for water reuse. Bioresour. Technol. 276, 226–235. doi:10.1016/j.biortech.2018.12.077.

Törnwall, E., Pettersson, H., Thorin, E., Schwede, S., 2017. Post-treatment of biogas digestate – An evaluation of ammonium recovery, energy use and sanitation. Energy Procedia 142, 957–963. doi:10.1016/j.egypro.2017.12.153.

Triques, C.C., Fagundes-Klen, M.R., Suzaki, P.Y.R., Mateus, G.A.P., Wernke, G., Bergamasco, R., et al., 2020. Influence evaluation of the functionalization of magnetic nanoparticles with a natural extract coagulant in the primary treatment of a dairy cleaning-in-place wastewater. J. Clean. Prod. 243. doi:10.1016/j.jclepro.2019.118634.

United States of Environmental Protection Agency, U., 2007. The Benefits of Anaerobic Digestion of Food Waste At Wastewater Treatment Facilities. EPA, USA.

Wan, T.J., Shen, S.M., Siao, S.H., Huang, C.F., Cheng, C.Y., 2011. Using magnetic seeds to improve the aggregation and precipitation of nanoparticles from backside grinding wastewater. Water Res 45, 6301–6307. doi:10.1016/j.watres.2011.08.067.

Wang, P., Jiao, R., Liu, L., Xiao, F., An, G., Wang, D., 2019. Optimized coagulation pathway of Al13: Effect of in-situ Aggregation of Al13. Chemosphere 230, 76–83. doi:10.1016/j.chemosphere.2019.05.053.

Xia, A., Murphy, J.D., 2016. Microalgal cultivation in treating liquid digestate from biogas systems. Trends Biotechnol. 34, 264–275. doi:10.1016/j.tibtech.2015.12.010.

Xiao, K., Han, B., Sun, J., Tan, J., Yu, J., Liang, S., et al., 2019. Stokes shift and specific fluorescence as potential indicators of organic matter hydrophobicity and molecular weight in membrane bioreactors. Environ. Sci. Technol. 53, 8985–8993. doi:10.1021/acs.est.9b02114.

Xiao, K., Sun, J.Y., Shen, Y.X., Liang, S., Liang, P., Wang, X.M., et al., 2016. Fluorescence properties of dissolved organic matter as a function of hydrophobicity and molecular weight: case studies from two membrane bioreactors and an oxidation ditch. RSC Adv. 6, 24050–24059. doi:10.1039/c5ra23167a.

Yoo, S.S., 2018. Operating cost reduction of in-line coagulation/ultrafiltration membrane process attributed to coagulation condition optimization for irreversible fouling control. Water (Switzerland) 10. doi:10.3390/w10081076.

Yu, J., Xiao, K., Xue, W., Shen, Y.X., Tan, J., Liang, S., et al., 2020. Excitation-emission matrix (EEM) fluorescence spectroscopy for characterization of organic matter in membrane bioreactors: Principles, methods and applications. Front. Environ. Sci. Eng. 14. doi:10.1007/s11783-019-1210-8.

Zhang, L.B., Tong, J., Wei, Y.S., Wang, J., Yue, Z.W., 2016. The progress of magnetic separation technology in water treatment. Acta Sci. Circumstantiae 36, 3103–3117 https://doi.org/DOI: 10.13671/j.hjkxxb.2015.0775.

Zhang, M., Xiao, F., Wang, D., Xu, X., Zhou, Q., 2017. Comparison of novel magnetic polyaluminum chlorides involved coagulation with traditional magnetic seeding coagulation: Coagulant characteristics, treating effects, magnetic sedimentation efficiency and floc properties. Sep. Purif. Technol. 182, 118–127. doi:10.1016/j.seppur.2017.03.028.

Zheng, L., Jiao, Y., Zhong, H., Zhang, C., Wang, J., Wei, Y., 2020. Insight into the magnetic lime coagulation-membrane distillation process for desulfurization wastewater treatment: From pollutant removal feature to membrane fouling. J. Hazard. Mater. 391, 122202. doi:10.1016/j.jhazmat.2020.122202.

Zheng, L., Yu, D., Wang, G., Yue, Z., Zhang, C., Wang, Y., et al., 2018. Characteristics and formation mechanism of membrane fouling in a full-scale RO wastewater reclamation process: Membrane autopsy and fouling characterization. J. Memb. Sci. 563, 843–856. doi:10.1016/j.memsci.2018.06.043.

Zhu, G., Bian, Y., Hursthouse, A.S., Xu, S., Xiong, N., Wan, P., 2020. The role of magnetic MOFs nanoparticles in enhanced iron coagulation of aquatic dissolved organic matter. Chemosphere 247, 125921. doi:10.1016/j.chemosphere.2020.125921.

Zsolnay, A., Baigar, E., Jimenez, M., Steinweg, B., Saccomandi, F., 1999. Differentiating with fluorescence spectroscopy the sources of dissolved organic matter in soils subjected to drying. Chemosphere 38, 45–50. doi:10.1016/S0045-6535(98)00166-0.

Zuriaga-Agustí, E., Mendoza-Roca, J.A., Bes-Piá, A., Alonso-Molina, J.L., Muñagorri-Mañueco, F., Ortiz-Villalobos, G., et al., 2016. Comparison between mixed liquors of two side-stream membrane bioreactors treating wastewaters from waste management plants with high and low solids anaerobic digestion. Water Res. 100, 517–525. doi:10.1016/j.watres.2016.05.053.